



Pb isotopic compositions of some Zn–Pb deposits and occurrences from Urumieh–Dokhtar and Sanandaj–Sirjan zones in Iran

H. Mirnejad^{a,*}, A. Simonetti^{b,c}, F. Molasalehi^a

^a Department of Geology, Faculty of Science, University of Tehran, Tehran, Iran

^b Department of Earth and Atmospheric Sciences, University of Alberta, Edmonton, Alberta, Canada T6G 2E3

^c Department of Civil Engineering & Geological Sciences, 156 Fitzpatrick Hall, University of Notre Dame, Notre Dame, IN 46556, USA

ARTICLE INFO

Article history:

Received 25 August 2010

Received in revised form 2 February 2011

Accepted 7 February 2011

Available online 21 March 2011

Keywords:

Pb isotopes

Neo-Tethys

Subduction

Zn–Pb deposits

Iran

ABSTRACT

This study reports Pb isotope ratios of galena (PbS) sampled from some Zn–Pb deposits and occurrences ($n = 18$) within two major structural provinces of Iran, the Sanandaj–Sirjan zone (SSZ) and Urumieh–Dokhtar zone (UDZ). Regardless of the nature of the host rock and ore type, the Pb isotopic data plot in distinct isotopic fields according to their geographic situation, which suggest that the structural terranes had an important control on the lead isotope compositions. The Zn–Pb deposits in the UDZ record distinctly higher $^{206}\text{Pb}/^{204}\text{Pb}$ and $^{208}\text{Pb}/^{204}\text{Pb}$ ratios compared to those within the SSZ. Both zones, however, have radiogenic $^{207}\text{Pb}/^{204}\text{Pb}$ ratios (> 15.55), suggesting a dominant input of Pb from crustal sources. In thorogenic ($^{208}\text{Pb}/^{204}\text{Pb}$ vs. $^{206}\text{Pb}/^{204}\text{Pb}$) and uraniumogenic ($^{207}\text{Pb}/^{204}\text{Pb}$ vs. $^{206}\text{Pb}/^{204}\text{Pb}$) plots, the Pb isotope data define two linear arrays, which may be attributed to mixing between mantle-like end members and at least two distinct crustal sources characterized by high U/Pb and Th/U ratios. In ‘Plumbotectonic’ discrimination diagrams, the samples plot proximal to the orogenic curve, which again supports interaction between crustal and mantle reservoirs. However, both Neo-Tethys subduction and in particular Mesozoic and Tertiary orogenic activities seem to have played important roles in remobilizing Pb and forming Zn–Pb deposits in SSZ and UDZ, respectively. The similarity of Pb isotopic compositions between UDZ deposits and those for previously reported Eocene volcanics demonstrates that long-lived and widespread hydrothermal activity promoted remobilization of lead from the crust; the latter occurred subsequent to Neo-Tethys lithosphere subduction in the Tertiary and continued subsequent the collision of the Iranian and Arabian plates in the Miocene.

© 2011 Elsevier B.V. All rights reserved.

1. Introduction

Pb isotopes are a powerful tool for understanding ore genesis and for the exploration of mineral deposits (e.g., Gulson, 1986). They are particularly useful in assessing the source of metals, providing important information about the nature of Pb reservoir(s), constraining the timing of Pb extraction from its source, and defining a geotectonic environment for ore deposits (e.g., Gariépy and Dupré, 1991). Galena (PbS) is the most suitable mineral for analysis of Pb isotope ratios within Zn–Pb deposits because it is essentially devoid of U and is characterized by an abundant Pb content (~87 wt.%); this combination ensures that its Pb isotopic composition remains unchanged throughout geologic time.

Information on the genesis and age of Zn–Pb ore deposits in Iran, particularly that available to international readers, is scarce. Even though many of these deposits are considered MVT (Mississippi-

Valley-Type; Ghorbani, 2002), considerable debate remains relative to the exact timing of mineralization and the source of the metals. Many of the Zn–Pb deposits in Iran have traditionally been considered to have formed during the Precambrian or Paleozoic (e.g., Samani, 1988), simply based on their spatial association with older country rocks. However, recent radiometric dating has yielded much younger ages for the Zn–Pb deposits; e.g., a Tertiary mineralization age (20 Ma) has been determined for the large Zn–(Pb–Ag) deposit at Anguran (Gilg et al., 2006). Lancelot et al. (1997) reported a Pb isotope study on galenas from several Iranian Zn–Pb ore deposits hosted by sedimentary formations, which include Anguran, Duna, Irankuh, Mehdiabad, and Nakllak; however detailed data for each deposit is lacking. Lancelot et al. (1997) stated that the deposits characterized by more radiogenic Pb isotope signatures (e.g., Anguran) are associated with older host rocks. This correlation strongly suggests that the extraction of Pb (and Pb–U fractionation) occurred within rocks from the upper continental crust. In addition, several models/hypotheses have been advocated in order to explain the formation of some of the Zn–Pb deposits in Iran. These include: 1 – syngenetic and epigenetic origin (Karimzadeh, 1992; Vanaei, 1998; Ziserman and Momenzadeh, 1972); 2 – remobilization and concentration of metals from metal-

* Corresponding author. Tel.: +98 21 6111 2959; fax: +98 21 6649 1623.

E-mail address: mirnejad@khayam.ut.ac.ir (H. Mirnejad).

bearing sediments (Momenzadeh and Rastad, 1973); 3 – submarine exhalative origin for the metals that were subsequently deposited in near-shore shallow water regime in the presence of organic material (Momenzadeh, 1976); 4 – MVT-type deposits (Ehya et al., 2010; Förster, 1978); 5 – hydrothermal solutions emanating from buried batholith at depth (Rahimpour-Bonab, 1991); 6 – mobilization of metals into host rocks following their concentration into veins (Shojaat, 1992).

Two major tectonic provinces, the Sanandaj–Sirjan zone (SSZ) and Urumieh–Dokhtar zone (UDZ), extending in a NW–SE direction across Iran (Fig. 1), were structurally modified as the result of the Neo-Tethys lithosphere subduction beneath Central Iran (Berberian and King, 1981). Both structural provinces are host to numerous Zn–Pb deposits and a significant number of major ore occurrences (~600; Ghorbani et al., 2000). For example, the Gol-Gohar magnetite deposit within the SSZ has an estimated reserve of 1135 million tons, and the Kerman porphyry copper deposit located within the UDZ is estimated to have a reserve of 1.1 Gt at a grade of 0.6% Cu (Fig. 1). In order to identify the ultimate source of Pb and to better understand the possible control of tectonic settings on the Pb isotopic nature of the Zn–Pb deposits in Iran, galena samples from Zn–Pb deposits from within the UDZ and SSZ structural zones have been analyzed for their Pb isotope compositions.

2. Geology

The geology of Iran is complex in large part because the continental crust consists of various microplates that were amalgamated during the opening and closure of both the Paleo-Tethys and Neo-Tethys oceans (Berberian and King, 1981; Stöcklin, 1977). It is believed that the Ordovician–Silurian opening of the Paleo-Tethys in northern Iran was followed by its northward subduction beneath the Turan plate (the southern part of Laurasia) in late Devonian, and the collision between the Iranian microcontinent and Turan plates in late Triassic–Jurassic (Natalin and Şengör, 2005; Stampfli, 2000). Following closure of the Paleo-Tethys, the Neo-Tethys oceanic crust was constructed and subducted below Central Iran in the Late Jurassic to Cretaceous (Mohajjel et al. (2003); Richards et al., 2006). The consumption of the Neo-Tethys ocean basin resulted in the collision of the Iranian and Arabian plates during the Oligocene–Miocene period (Berberian and King, 1981; Stampfli, 2000; Stöcklin, 1977). The effects of Paleo-Tethys subduction in Iran are not well documented because the current suture zone is located in the vicinity of the northern geographical borders. In contrast, the Neo-Tethys subduction is well characterized because of its location along the Zagros orogenic belt that extends throughout the country from NW to SE of Iran (Fig. 1). The Zagros orogenic belt is part of the Alpine–Himalayan orogenic belt, which extends from Europe,

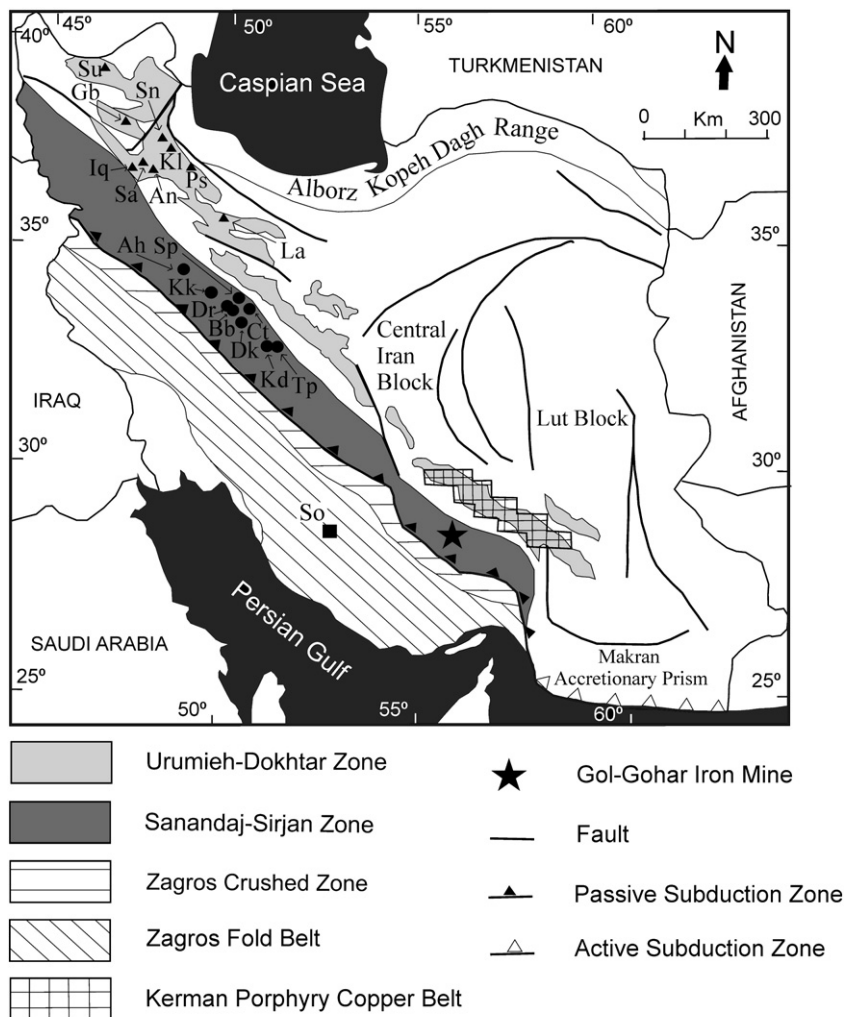


Fig. 1. Map showing sample locations and the position of the Urumieh–Dokhtar and Sanandaj–Sirjan zones relative to other structural zones of Iran (modified after Daliran, 2008; Gilg et al., 2006; Stöcklin, 1968). Sample abbreviations are given in Table 1.

through Iran, to western Pakistan. From SW to NE four main structural units are recognized across the Zagros (Fig. 1): Zagros fold belt, Zagros crushed zone, the Sanandaj–Sirjan zone (SSZ), and the Urumieh–Dokhtar zone (UDZ) (Agard et al., 2005; Alavi, 1994; Berberian and King, 1981; Bina et al., 1986; Braud and Ricou, 1971; Stöcklin, 1977). It has been proposed that the metamorphic and igneous rocks in the SSZ formed during various stages of Neo-Tethys subduction in early to late Mesozoic times (Ghalamghash et al., 2009; Ghasemi and Talbot, 2006; Mohajjel et al., 2003; Richards et al., 2006; Wrobel–Daveau et al., 2010). Subduction of the Neo-Tethys lithosphere beneath Central Iran resulted in the formation of the UDZ, a volcano-plutonic calc-alkaline belt (parallel to the SSZ) consisting predominantly of Tertiary intrusive and extrusive rocks (Agard et al., 2005; Omrani et al., 2008; Richards et al., 2006). Although the UDZ hosts many porphyry copper deposits in its SE region, the Zn–Pb deposits are mainly concentrated in the NW section of the zone (Fig. 1). One of the Zn–Pb deposits from the latter region investigated here has been sampled from a Tertiary porphyry Cu deposit (Sungun), whereas most of the remaining samples occur as veins in the Tertiary volcanic rocks (Table 1). The SSZ hosts a number of large Zn–Pb deposits predominantly within Mesozoic sedimentary rocks (e.g. Emarat; Ehya et al., 2010). In general, the majority of the Zn–Pb deposits from UDZ are of the vein-type, while those of the SSZ are MVT/exhalative-type. Compared to the UDZ and SSZ, the Zagros fold belt does not contain significant amounts of ore deposits, and the Kuh-e Sormeh deposit is the only known Zn–Pb deposit in this zone (Fig. 1). According to Liaghat et al. (2000), Kuh-e Sormeh is an orogen-related MVT deposit originally formed in the foreland Thrust Belt of the Zagros Mountains. The strata exposed in the Kuh-e Sormeh district include almost complete sections of Paleozoic, Mesozoic and Cenozoic sediments (Ghavidel–Syooki, 1995; James and Wynd, 1965).

3. Sampling and methodology

Eighteen fresh galena samples representative of Zn–Pb deposits from SSZ and UDZ as well as one sample from Zagros fold belt were collected on field trips during the summer of 2007. Table 1 lists their description and Fig. 1 shows the locations of the sampling sites. Galena separates were carefully handpicked to avoid inclusions from surrounding minerals. 2–3 mg of sample was dissolved using ultrapure (double distilled) HCl. Pb isotope compositions were analyzed using a multicollector-inductively coupled plasma mass spectrometer (MC-ICP-MS) instrument (Nu Instruments Ltd, Wrexham, UK) within the Radiogenic Isotope facility at the University of Alberta. Sample aliquots were subsequently mixed with ~1.5 mL of a 2% HNO₃ solution spiked with the NIST SRM 997 Thallium standard (2.5 ppb), and aspirated (~100 µL/min) into the ICP source using an ARIDUS microconcentric nebulizer (Nu Instruments Ltd). The analytical protocol for Pb isotope measurement outlined below follows the procedure described in Simonetti et al. (2004).

Simultaneous measurement of all the Pb and Tl isotopes, and ²⁰²Hg ion signal was achieved by using seven Faraday collectors. The ²⁰⁵Tl/²⁰³Tl ratio was measured to correct for instrumental mass bias (exponential law; ²⁰⁵Tl/²⁰³Tl = 2.3871). Upon sample introduction, data acquisition consisted of 2 half-mass unit baseline measurements prior to each integration block, and 3 blocks of 20 scans (10 s integration each) for isotope ratio analysis. ²⁰⁴Hg interference (on ²⁰⁴Pb) was monitored and corrected using ²⁰²Hg. At the beginning of the analytical session, a 25 ppb solution of the NIST SRM 981 Pb standard, which was also spiked with the NIST SRM 997 Tl standard (1.25 ppb), was analyzed. External reproducibility of the protocol was evaluated via repeated measurement (n = 3) of the NIST SRM 981

Table 1
Sample information for galenas from Zn–Pb deposits examined in this study.

Sample #	Deposit name	Deposit description	Ore type
SSZ			
^a Ah	Ahangaran	Massive and veinlet sulfide in faults and fractures of Lower Cretaceous carbonate units	Exhalative Momenzadeh (1976), Zamanian (1993)
Kk	Koh Kolangeh	Massive and veinlet sulfide in faults and fractures of Lower Cretaceous limestone and marly limestone	Exhalative Momenzadeh (1976)
^a Tp	Tapesorkh	Fault and fractures infilling of Lower Cretaceous carbonate units	MVT? Exhalative?
^a Kd	Kolahdarvazeh	Karst, faults and fractures which are branched from major faults in Lower Cretaceous limestone and marly limestone	MVT Ghasemi Todshkchoii (1995)
Dk	Doshkharat	Fault and fractures infilling of Lower Cretaceous	MVT? Exhalative?
Dr	Darenoghreh	Veins in Lower Cretaceous limestone	MVT? Exhalative?
Bb	Babasheykh	Vein in Lower Cretaceous carbonaceous-clastic units	MVT? Exhalative?
Ct	Chahtalkh	Fracture infilling of Lower Cretaceous marly limestone	MVT? Exhalative?
Sp	Salehpeighambar	Disseminated and fracture infilling within Lower Cretaceous limestone	MVT? Exhalative?
UDZ			
^a An	Anguran	Brecciated and massive minerals in Neoproterozoic–Cambrian metamorphic rocks (micaschist, amphibolite and marble)	Low-temperature carbonate-hosted Zn–Pb ore Gilg et al. (2006)
Sa	Saryaghol	Vein and breccia in Oligocene–Miocene carbonates	MVT? Vein?
Ps	Pasar	Vein and veinlet in Eocene volcanic rocks	Vein
Iq	Iqalesi	Vein and veinlet in silica zone in Oligocene–Miocene (?) quartz diorite intrusion	Vein
^a Su	Sungon	Vein and veinlet around porphyry copper deposit in Miocene granodioritic intrusion	Vein
La	Lak	Vein and veinlet associated with fault zone in Eocene volcanic rocks	Vein
Sn	Senjedeh	Pb, Zn bearing veins and veinlets system in Eocene andesitic and rhyolitic tuff	Vein
Kl	Khalf	Vein and veinlet in Eocene andesitic and rhyolitic tuff	Vein
Gb	Ghebchagh	Vein and veinlet in silica zone in Eocene volcanic rocks	Vein
ZFB			
^a So	Kohe Sormeh	Massive, open space and fracture filling in Permian carbonate units	MVT Liaghat et al. (2000)

SSZ = Sanandaj–Sirjan zone, UDZ = Urumieh–Dokhtar zone, ZFB = Zagros fold belt.

^a Deposits which are currently mined for Zn and/or Pb ore.

Table 2
Pb isotope compositions of the analyzed samples.

Sample	$^{206}\text{Pb}/^{204}\text{Pb}$	$^{207}\text{Pb}/^{204}\text{Pb}$	$^{208}\text{Pb}/^{204}\text{Pb}$	μ ($^{238}\text{U}/^{204}\text{Pb}$)	k ($^{232}\text{Th}/^{238}\text{U}$)
SSZ					
Ahangaran (Ah)	18.407 ± 0.003	15.641 ± 0.003	38.571 ± 0.011	9.858	3.95
Kohkolangeh (Kk)	18.389 ± 0.004	15.628 ± 0.005	38.470 ± 0.014	9.806	3.903
Tapeh Sorkh (Tp)	18.450 ± 0.003	15.651 ± 0.003	38.627 ± 0.009	9.893	3.955
Kolah darvazeh (Kd)	18.419 ± 0.002	15.634 ± 0.002	38.562 ± 0.007	9.825	3.934
Doshkharat (Dk)	18.440 ± 0.002	15.659 ± 0.002	38.642 ± 0.006	9.929	3.931
Dareh noghreh (Dr)	18.398 ± 0.003	15.640 ± 0.003	38.488 ± 0.010	9.857	3.911
Babasheikh (Bb)	18.424 ± 0.004	15.646 ± 0.004	38.539 ± 0.014	9.875	3.923
Chah talkh (Ct)	18.454 ± 0.005	15.635 ± 0.002	38.600 ± 0.007	9.819	3.931
Saleh peighambar (Sp)	18.471 ± 0.005	15.652 ± 0.006	38.650 ± 0.017	9.891	3.953
UDZ					
Angouran (An)	18.919 ± 0.005	15.702 ± 0.005	38.911 ± 0.015	10.01	3.815
Saryaghol (Sa)	18.667 ± 0.005	15.652 ± 0.006	38.736 ± 0.018	9.845	3.868
Pasar (Ps)	18.735 ± 0.011	15.648 ± 0.010	38.755 ± 0.025	9.812	3.832
Iqalesi (Iq)	18.843 ± 0.004	15.669 ± 0.004	38.861 ± 0.012	9.916	3.828
Sungun (Su)	18.831 ± 0.003	15.654 ± 0.003	38.933 ± 0.009	9.822	3.863
Lak (La)	18.647 ± 0.004	15.606 ± 0.003	38.668 ± 0.008	9.653	3.828
Senjehdeh (Sn)	18.730 ± 0.003	15.628 ± 0.003	38.788 ± 0.008	9.731	3.845
Khalf (Kl)	18.722 ± 0.002	15.617 ± 0.002	38.761 ± 0.007	9.684	3.832
Ghebchagh (Gb)	18.867 ± 0.003	15.634 ± 0.003	38.901 ± 0.008	9.738	3.817
ZFB					
Kuh-e Sormeh (So)	18.062 ± 0.004	15.684 ± 0.004	38.230 ± 0.012	10.157	4.017

Individual errors represent within run uncertainties at the 2 sigma level.

standard solution and yielded the following mean values and associated (2σ) standard deviations: $^{206}\text{Pb}/^{204}\text{Pb} = 16.936 \pm 0.006$, $^{207}\text{Pb}/^{204}\text{Pb} = 15.489 \pm 0.004$, $^{208}\text{Pb}/^{204}\text{Pb} = 36.690 \pm 0.009$, $^{207}\text{Pb}/^{206}\text{Pb} = 0.91457 \pm 0.00012$, and $^{208}\text{Pb}/^{206}\text{Pb} = 2.1664 \pm 0.0003$.

4. Results

The Pb isotope data for the galena samples investigated here are listed in Table 2. $^{206}\text{Pb}/^{204}\text{Pb}$, $^{207}\text{Pb}/^{204}\text{Pb}$ and $^{208}\text{Pb}/^{204}\text{Pb}$ ratios for galenas from the SSZ range from 18.389 to 18.471, 15.628 to 15.659, and 38.47 to 38.650, respectively. Galenas from UDZ are characterized by more radiogenic $^{206}\text{Pb}/^{204}\text{Pb}$ and $^{208}\text{Pb}/^{204}\text{Pb}$ ratios, and range from 18.647 to 18.919 and 38.668 to 38.911, respectively. Samples from the Anguran and Soulakhan (Gilg et al., 2006) and Emarat (Ehya et al., 2010) Zn–Pb deposits are also characterized by distinct radiogenic Pb isotope ratios, similar to other Zn–Pb deposits from the UDZ and SSZ, respectively. In the Pb–Pb isotope diagram (Fig. 2), the data for Zn–Pb deposits from SSZ and UDZ as well as the sole sample from the Zagros fold belt plot in distinct compositional fields (Fig. 2). Moreover, the Pb isotope data define two distinct positive correlations on the thorogenic diagram ($^{208}\text{Pb}/^{204}\text{Pb}$ vs. $^{206}\text{Pb}/^{204}\text{Pb}$). While the data are seemingly more scattered on the uranogenic diagram ($^{207}\text{Pb}/^{204}\text{Pb}$ vs. $^{206}\text{Pb}/^{204}\text{Pb}$), which most probably results from the larger uncertainty involved with the measurement of the $^{207}\text{Pb}/^{204}\text{Pb}$ ratios, these do also form well-defined linear arrays.

Fig. 3 shows the growth curves for the Doe and Zartman (1979) Plumbotectonics model. Pb isotope data from both SSZ and UDZ plot between the orogen and lower crust evolution curves in the thorogenic diagram (Fig. 3a), and between the orogen and upper crust growth curves in the uranogenic plot (Fig. 3b). The Pb isotopic compositions of sulfide separates from the porphyry copper deposits in UDZ (Shafiei, 2010; Shahabpour and Kramers, 1987) also plot between the orogen and crustal growth curves (Fig. 3). Of interest, the SSZ Zn–Pb deposits define a tighter cluster of points compared to the data from the UDZ (Fig. 3).

5. Discussion

The Pb isotope data for the samples investigated here exhibit positive correlations in both Pb–Pb isotope plots, in particular for the thorogenic diagram (Fig. 2), which may be considered mixing lines. Therefore, these may reflect mixing between multiple end-members. The existence of a correlation between geographic location (i.e., SSZ vs. UDZ) and Pb isotope values suggests that the linear arrays in Figs. 2 and 3 may result from the contamination of Pb derived from mantle-like (e.g. mantle ± crust modified) sources with Pb of variable composition

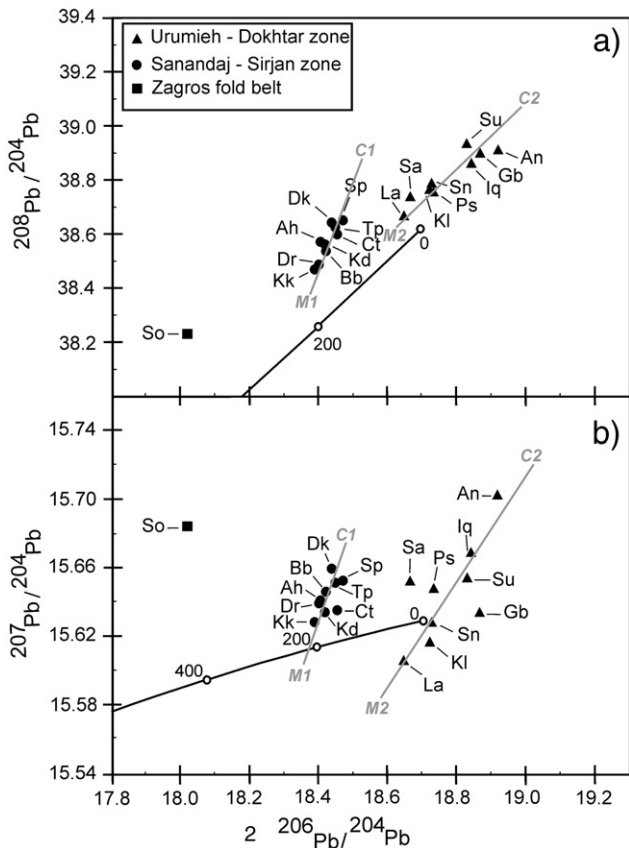


Fig. 2. Variations of $^{207}\text{Pb}/^{204}\text{Pb}$ vs. $^{206}\text{Pb}/^{204}\text{Pb}$ and $^{208}\text{Pb}/^{204}\text{Pb}$ vs. $^{206}\text{Pb}/^{204}\text{Pb}$ for the studied samples. Numbers on the Stacey–Kramers growth line (Stacey and Kramers, 1975) indicate ages in Ga. The lines defined by the SSZ and UDZ characterize mixing between mantle-like sources (M1 and M2) and two different crustal sources (C1 and C2). Sample abbreviations are given in Table 1.

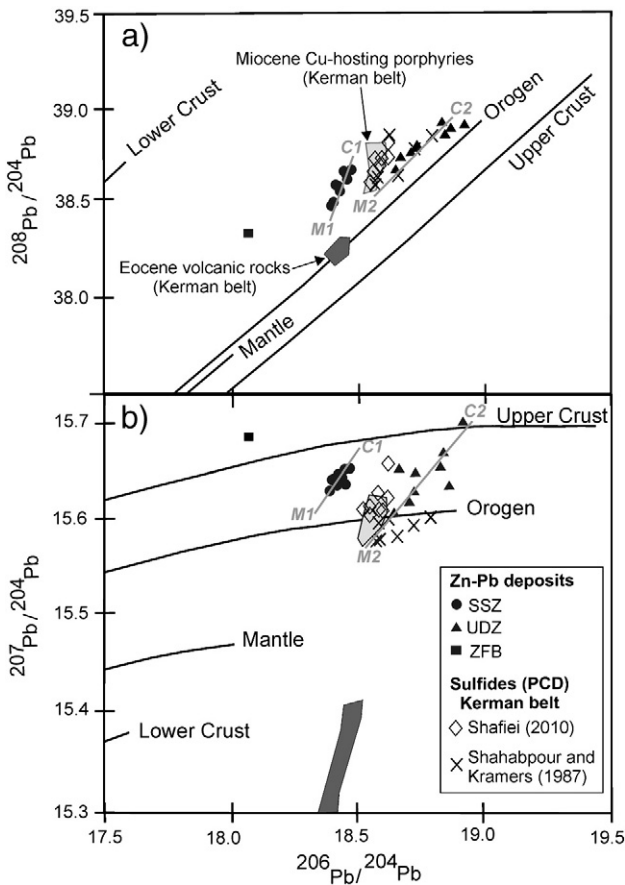


Fig. 3. Pb isotope ratios of analyzed samples on the 'plumbotectonic' diagram (Doe and Zartman, 1979). Pb isotope data for sulfide separates from Kerman porphyry copper deposits (PCD), their Miocene ore-hosting porphyries and surrounding Eocene volcanic rocks (Shahabpour and Kramers, 1987; Shafiei, 2010) are given for comparison.

from the crustal basement rocks. The latter refer to the basement proper, as well as the overlying column of crustal rocks traversed by hydrothermal solutions. The Pb isotope compositions for the galenas may well reflect those of the lithologies surrounding or underlying the deposits since the Zn–Pb deposits from the SSZ (hosted predominantly by the sedimentary rocks) have distinct Pb isotope signatures compared to those from the UDZ (hosted primarily by volcanic rocks). Also noteworthy is the fact that the mixing lines defined by the SSZ and UDZ galena samples in the thorogenic and uranium diagrams (Fig. 2) are characterized by different slopes, which are probably indicative of both distinct sources and ages of mineralization. The least radiogenic end members for the mixing lines most likely represent a mantle-like component. In Fig. 3, the regression lines defined by the UDZ data intersect (at the least radiogenic end) very close to the whole rock Pb isotope compositions for the Eocene volcanic rocks within the Kerman Cenozoic magmatic arc (KMCA; Shafiei, 2010). Thus, it is possible that a similar mantle-like end-member that was involved in the generation of the porphyry copper deposits of the KMCA (Shafiei, 2010) was also the source of (mantle) Pb for the Zn–Pb deposits in the UDZ. However, the SSZ and UDZ deposits have distinct $^{206}\text{Pb}/^{204}\text{Pb}$ ratios with respect to their least radiogenic values, which indicate that the 'mantle-like' Pb in these two structural zones was not derived from the same source. This interpretation is supported by the geodynamic histories for these two structural zones since magmatism did not occur concomitantly; i.e. in relation to the Neo-Tethys subduction, magmatism took place in the Mesozoic within the SSZ and in the Tertiary for the UDZ. This is consistent with the more radiogenic composition of the younger (Tertiary) mantle magmatic component of the UDZ deposits (component M2 in Fig. 2) compared to

the less radiogenic composition of the older (Mesozoic) mantle magmatic component of the SSZ deposits (component M1 in Fig. 2).

The Pb isotope data from the UDZ and SSZ Zn–Pb deposits also plot very close to the average orogen curve of Doe and Zartman (1979). This feature suggests the incorporation of crustal-derived Pb during their formation, although the exact source for the Pb remains unclear due to the lack of Pb isotope characterization of crustal components in the region. The variations in the Pb isotope ratios for sulfide separates from the Kerman belt porphyry copper deposits in the UDZ, which resemble those of their host porphyries (Fig. 3), were interpreted as derivation of Pb from a mantle-derived magmatic source, largely influenced by crustal material (Shafiei, 2010; Shahabpour and Kramers, 1987). For the Zn–Pb deposits investigated here, those exhibiting the most radiogenic compositions, characterized by high μ and k values (Table 2), necessitate the involvement of a crustal source. A dominant continental crust origin for the Pb is also evidenced by the high $^{207}\text{Pb}/^{204}\text{Pb}$ ratios (>15.59) in both UDZ and SSZ Zn–Pb deposits (Fig. 2b). These observations are interpreted to indicate that the mantle-derived magma genetically related to the Neo-Tethys subduction produced the hydrothermal system, which remobilized crustal Pb and formed the deposit. Moreover, the SSZ deposits are characterized by a narrow range of $^{207}\text{Pb}/^{204}\text{Pb}$ and $^{206}\text{Pb}/^{204}\text{Pb}$ values, whereas those for the UDZ deposits are much more variable (Fig. 3). This result is consistent with different mantle–crust mixing processes in the UDZ and SSZ terranes. On the basis of the Pb isotope data (Figs. 2 and 3), calculated Th/Pb and U/Pb ratios for the radiogenic end-member are high, indicative that crustal material also played an important role in the formation of the SSZ and UDZ deposits. More specifically, the Pb isotope values for the SSZ deposits define a steeper mixing line, compared to the Pb isotope signatures for the UDZ deposits; the latter define a trend sub parallel to the upper crust/orogenic-like component (Fig. 2). These features most probably reflect the distinct compositions of the 'basement' associated with each zone; however, additional Pb isotope data are needed to fully and accurately explain these systematic differences in Pb isotope values. The basement rocks would then impart their Pb isotopic signature on the hydrothermal fluids forming the Zn–Pb deposits. Given the contrasting geodynamic histories of the Neo-Tethys, it is not surprising to assume that the SSZ is characterized by crust of a lesser-radiogenic nature, whereas the UDZ consists predominantly of a more radiogenic crustal reservoir. The basement rocks in the SSZ experienced moderate-to-high degree of metamorphism (greenschist \pm amphibolite facies) during the Mesozoic Cimmerian orogeny (Baharifar et al., 2004; Berberian and King, 1981; Mohajjel and Fergusson, 2000) as the result of the Neo-Tethys subduction beneath Central Iran. Moreover, eclogitic lenses or blocks occurring within the ortho- and paragneisses north of Shahrekord within the SSZ have been attributed to an eclogite facies metamorphic event (Davoudian et al., 2008). It is documented that moderate-to-high degrees of metamorphism can be accompanied by U-depletion (Downes et al., 2001; Kalsbeek, 1974; Whitehouse, 1989). In contrast, the UDZ did not undergo such high-grade metamorphic activity associated with possible U-depletion because of its remote distance to the Neo-Tethys ocean trench.

The distinct nature of the Pb isotope data from UDZ and SSZ (Fig. 3) can be attributed not only to the different mixing processes between the above mentioned reservoirs within the distinct structural terranes, but also to the time at which the mixing/mineralization occurred. The Pb isotope data from Kuh-e Sormeh, the sole Zn–Pb deposit in the Zagros fold belt located to the SW of the suture zone and thus not affected by the Neo-Tethys orogenic activity, has the highest μ and k values (Table 2). Kuh-e Sormeh's Pb model age (585 Ma) is substantially older than its Upper Permian carbonate host rocks (Liaghat et al., 2000); however, this age correlates well with the Pan-African tectonic event and the late-Precambrian cratonization of the Iranian and Arabian plates during their amalgamation to the NE part of Gondwana (Stöcklin, 1968). This result, along with the differences in the mode and time of formations for the SSZ and UDZ indicates that

the tectonic setting exerted an important control on the Pb isotope compositions of Zn–Pb deposits in Iran. On the basis of the Pb isotope data shown in the 'plumbotectonic' diagrams (Fig. 3), it is quite likely that both the Zn–Pb and Cu mineral deposits within the UDZ formed during Tertiary magmatic arc-related activities. Ceyhan (2003) investigated the Pb isotopic compositions of galenas from Zn–Pb deposits in the eastern Taurides (southern Turkey), and noted that the data defined a similar outline (on Pb–Pb plots) to those from the Anguran deposit in the UDZ. Previous studies of the igneous rocks from both the SSZ and UDZ reveal that these formed mainly during two distinct episodes of magmatic activity that occurred during the Mesozoic and Tertiary, respectively (Agard et al., 2005; Ghalamghash et al., 2009; Mohajjel et al., 2003). This feature suggests that the axis of magmatism shifted ~300 km to the northeast from its initial position within the SSZ at the end of the Mesozoic. The geochemical signatures of the Mesozoic and Tertiary igneous rocks from both the SSZ and UDZ are very similar with no continuous suture zone present between them. This led Omrani et al. (2008) and Verdel (2009) to conclude that magmatism shifted from the SSZ to the UDZ in the late Cretaceous as the result of the flat-slab subduction of the Neo-Tethys. The grouping of the Pb isotope data based on their structural zones (Fig. 3) also suggests two distinct episodes of mineralization such that many Zn–Pb deposits in SSZ formed intermittently during the earlier stage of Neo-Tethys subduction; whereas those in UDZ formed at a later time during advanced stages of subduction, or early stages of continental collision.

In general, Pb isotope compositions obtained for Zn–Pb deposits have been used for terrane discrimination purposes (e.g., Chiaradia et al., 2004; Franklin et al., 1983; Gunnesch et al., 1990; Puig, 1988). Thus, as explained above, differences in the Pb isotope systematics for deposits within the UDZ and SSZ can most probably be attributed to regional and temporal differences in the Pb composition of the mantle and basement. The latter would then impart their Pb isotope signals to the hydrothermal fluids giving rise to the deposits. Therefore, it is expected that all of the Zn–Pb deposits within the SSZ and UDZ (including those that have yet to be analyzed) plot proximal to the M1–C1 and M2–C2 trend lines on the thorogenic and uranogenic diagrams (Fig. 2), respectively. For example, the Anguran Zn–(Pb–Ag) deposit has previously been attributed to either the SSZ or the UDZ (e.g., Boni et al., 2007; Daliran, 2008; Gilg et al., 2006); however, based on its proximal position to the 'UDZ' mixing (trend) lines in the Pb isotope diagrams (Fig. 2), it is clear that the source of Pb for this deposit was within the UDZ. The very radiogenic Pb isotopic nature of the galenas from the Anguran deposit may be the result of interaction between mantle-derived Pb and that from a radiogenic crustal component.

Lead isotope compositions for the Zn–Pb deposits from the SSZ are relatively uniform and plot in a tighter cluster compared to the data from the UDZ (Fig. 2). This result may reflect a more efficient mechanism for homogenizing the uranogenic isotopic compositions in the source areas and/or during the mineralization of the SSZ.

6. Conclusions

Pb isotope analyses for galena retrieved from Zn–Pb deposits within two important structural provinces in Iran, SSZ and UDZ, indicate that the deposits within the UDZ are characterized by distinctively higher $^{208}\text{Pb}/^{204}\text{Pb}$ and $^{206}\text{Pb}/^{204}\text{Pb}$ ratios compared to those within the SSZ. In the thorogenic and uranogenic diagrams, the data from the SSZ and UDZ define positive arrays/trends with different slopes. Our preferred interpretation is that mixing occurred between multiple mantle-like sources and at least two distinct crustal end-members. The less radiogenic nature (lower $^{208}\text{Pb}/^{204}\text{Pb}$ and $^{206}\text{Pb}/^{204}\text{Pb}$ ratios) of the Pb isotope compositions for the Zn–Pb deposits from the SSZ are consistent with interaction with unradiogenic crustal basement rocks. In contrast, hydrothermal fluids that

generated the Zn–Pb deposits from the UDZ seem to have interacted with more radiogenic crustal rocks. The geographic control of the Pb isotope compositions also suggests the Zn–Pb deposits of SSZ and UDZ were derived from not only different source regions but also related to distinct metallogenic events. Thus, we interpret the formation of Zn–Pb deposits in both the SSZ and UDZ to be the result of remobilization of Pb during orogenic activity related to the Neo-Tethys subduction beneath the Iranian plate. Mantle-derived magmas genetically related to the Neo-Tethys subduction helped establish the hydrothermal system, which subsequently remobilized crustal Pb and formed the individual deposits.

Acknowledgments

We thank Dr. H. A. Gilg for his editorial handling and constructive comments, and Dr. J. Richards and an anonymous reviewer for detailed and insightful comments.

References

- Agard, P., Omrani, J., Jolivet, L., Mouthereau, F., 2005. Convergence history across Zagros (Iran): constraints from collisional and earlier deformation. *International Journal of Earth Sciences* 94, 401–419.
- Alavi, M., 1994. Tectonics of Zagros Orogenic belt of Iran, new data and interpretation. *Tectonophysics* 229, 211–238.
- Baharifar, A., Moinevaziri, H., Bellon, H., Piqué, A., 2004. The crystalline complexes of Hamadan (Sanandaj–Sirjan zone, western Iran): metasedimentary Mesozoic sequences affected by Late Cretaceous tectono-metamorphic and plutonic events. *Comptes Rendus Geoscience* 336, 1443–1452.
- Berberian, M., King, G.C.P., 1981. Towards a paleogeography and tectonic evolution of Iran. *Canadian Journal of Earth Sciences* 18, 210–265.
- Bina, M.M., Bucur, I., Pervot, M., Meyerfeld, Y., Daly, L., Cantagrel, J.M., Mergoil, J., 1986. Palaeomagnetism petrology and geochronology of Tertiary magmatic and sedimentary units from Iran. *Tectonophysics* 121, 303–329.
- Boni, M., Gilg, H.A., Balassone, G., Schneider, J., Allen, C.A., Moore, F., 2007. Hypogene Zn carbonate ores in the Angouran deposit, NW Iran. *Mineral Deposita* 42, 799–820.
- Braud, J., Ricou, L.E., 1971. L'accident du Zagros ou Main Thrust un charriage et un coulissement. *Comptes Rendus Acad Science* 272, 203–206.
- Ceyhan, N., 2003. Lead isotope geochemistry of Pb–Zn deposits from Eastern Taurides, Turkey. M. Sc. Thesis. Department of Geological Engineering, The Middle East Technical University, Ankara, Turkey. 90 pp.
- Chiaradia, M., Fontboté, L., Paladines, A., 2004. Metal sources in mineral deposits and crustal rocks of Ecuador (1° N–4° S): a lead isotope synthesis. *Economic Geology* 99, 1085–1106.
- Daliran, F., 2008. The carbonate rock-hosted epithermal gold deposit of Agdarreh, Takab geothermal field, NW Iran—hydrothermal alteration and mineralization. *Mineralium Deposita* 43, 383–404.
- Davoudian, A.R., Genser, J., Dachs, E., Shabaniyan, N., 2008. Petrology of eclogites from north of Shahrekord, Sanandaj–Sirjan Zone, Iran. *Mineralogy and Petrology* 92, 393–413.
- Doe, B.R., Zartman, R.E., 1979. Plumbotectonics I: the Phanerozoic. In: Barnes, H.L. (Ed.), *Geochemistry of Hydrothermal Ore Deposits*, 2nd ed. John Wiley and Sons, pp. 22–70.
- Downes, H., Markwick, A.J.W., Kempton, P.D., Thirlwall, M.F., 2001. The lower crust beneath cratonic north-east Europe: isotopic constraints from garnet granulite xenoliths. *Terra Nova* 13, 395–400.
- Ehya, F., Lotfi, M., Rasa, I., 2010. Emarat carbonate-hosted Zn–Pb deposit, Markazi Province, Iran: a geological, mineralogical and isotopic (S, Pb) study. *Journal of Asian Earth Sciences* 37, 186–194.
- Förster, H., 1978. Mesozoic–Cenozoic metallogenesis in Iran. *Journal of the Geological Society of London* 135, 443–455.
- Franklin, J.M., Roscoe, S.M., Loveridge, W.D., Sangster, D.F., 1983. Lead isotope studies in Superior and southern provinces. *Geological Survey of Canada Bulletin* 351 60 pp.
- Gariépy, C., Dupré, B., 1991. Pb isotopes and crust–mantle evolution. In: Heaman, L., Ludden, J.N. (Eds.), *Short Course Handbook on Applications of Radiogenic Isotope Systems to Problems in Geology*. Mineralogical Association of Canada, pp. 191–224.
- Ghalamghash, J., Nédélec, A., Bellon, H., Vousoughi Abedini, M., Bouchez, J.L., 2009. The Urumieh plutonic complex (NW Iran): a record of the geodynamic evolution of the Sanandaj–Sirjan zone during Cretaceous times — Part I: petrogenesis and K/Ar dating. *Journal of Asian Earth Sciences* 35, 401–425.
- Ghasemi Todshkchoi, A., 1995. Geology and geochemistry of Kolah–Darvazeh and Godzandan Zn–Pb deposits in southern flanks of Irankuh, Southwest Isfahan. M. Sc. thesis. Tarbiat Modares University, Tehran (In Farsi).
- Ghasemi, A., Talbot, C.J., 2006. A new tectonic scenario for the Sanandaj–Sirjan Zone (Iran). *Journal of Asian Earth Sciences* 26, 683–693.
- Ghavidel-Syooki, M., 1995. Palynological study and age determination of the Ordovician sediments and Faraghan formation in Kuh-e-Surmeh at southern Iran. *Earth Science Magazine* 3, 29–35 (in Farsi).
- Chorbani, M., 2002. An introduction to economic geology of Iran. *National Geosciences Database of Iran. Report No. 2*. 695 pp. (in Farsi).

- Ghorbani, M., Tajbakhsh, P., Khoii, N., 2000. Pb–Zn deposits of Iran. Geological Survey of Iran. 512 pp.
- Gilg, H.A., Boni, M., Balassone, G., Allen, C.R., Banks, D., Moore, F., 2006. Marble-hosted sulfide ores in the Anguran Zn–(Pb–Ag) deposit, NW Iran: interaction of sedimentary brines with a metamorphic core complex. *Mineralium Deposita* 41, 1–16.
- Gulson, B.L., 1986. Lead Isotopes in Mineral Exploration. Elsevier Science Publishers, Amsterdam. 245 pp.
- Gunnesch, K.A., Baumann, A., Gunnesch, M., 1990. Lead isotope variations across the Central Peruvian Andes. *Economic Geology* 85, 1384–1401.
- James, G.A., Wynd, J.G., 1965. Stratigraphic nomenclature of Iranian Oil Consortium agreement area. *American Association of Petroleum Geologist Bulletin* 49, 2182–2245.
- Kalsbeek, F., 1974. U, Th and K contents and metamorphism of Archaean rocks from south-west Greenland. *Bulletin of the Geological Society of Denmark* 23, 124–129.
- Karimzadeh, A., 1992. Investigation on type, mineralogical–geochemical relationships, and the possible genesis of Emarat lead–zinc mine (Arak). M. Sc. Thesis, Tarbiat Moallem University, Tehran, Iran (In Farsi).
- Lancelot, J., Orgeval, J.J., Fariss, K., Zadeh, H., 1997. Lead isotope signature of major Iranian Zn–Pb ore deposits (Anguran, Duna, Irankuh, Mehdiabad, Nakllak). *Terra Nova* 9, 550 Abstract Supplement 1.
- Liaghat, S., Moore, F., Jami, M., 2000. The Kuh-e Surmeh mineralization, a carbonate hosted Zn–Pb deposit in the simply folded belt of the Zagros Mountains, SW Iran. *Mineralium Deposita* 35, 72–78.
- Mohajjel, M., Fergusson, C.L., 2000. Dextral transpression in late Cretaceous continental collision, Sanandaj–Sirjan Zone, Western Iran. *Journal of Structural Geology* 22, 1125–1139.
- Mohajjel, M., Fergusson, C.L., Sahandi, M.R., 2003. Cretaceous–Tertiary convergence and continental collision, Sanandaj–Sirjan Zone, western Iran. *Journal of Asian Earth Sciences* 21, 397–412.
- Momenzadeh, M., 1976. Stratabound lead–zinc ores in the Lower Cretaceous and Jurassic sediments in the Malayer–Esfahan district (west central Iran), lithology, metal content, zonation and genesis. Ph.D. Thesis, Heidelberg University.
- Momenzadeh, M., Rastad, E., 1973. Zinc, lead and iron mineralization in Cretaceous carbonatic rocks in the West-Central Iran metallogenic zone. Geological Survey of Iran 4 In Farsi.
- Natalin, B.A., Şengör, A.M., 2005. Late Palaeozoic to Triassic evolution of the Turan and Scythian platforms: the pre-history of the Palaeo-Tethyan closure. *Tectonophysics* 404, 175–202.
- Omrani, J., Agard, P., Whitechurch, H., Benoit, M., Prouteau, G., Jolivet, L., 2008. Arc-magmatism and subduction history beneath the Zagros Mountains, Iran: a new report of adakites and geodynamic consequences. *Lithos* 106, 380–398.
- Puig, A., 1988. Geologic and metallogenic significance of the isotopic composition of lead in galenas of the Chilean Andes. *Economic Geology* 83, 843–858.
- Rahimpour-Bonab, H., 1991. Investigation on lead–zinc deposits of South of Arak region (Emarat). M. Sc. Thesis. University of Tehran, Tehran, Iran (In Farsi).
- Richards, J.P., Wilkinson, D., Ullrich, T., 2006. Geology of the Sari Gunay Epithermal Gold Deposit, Northwest Iran. *Economic Geology* 101, 1455–1496.
- Samani, B.A., 1988. Metallogeny of the Precambrian in Iran. *Precambrian Research* 39, 85–106.
- Shafiei, B., 2010. Lead isotope signatures of the igneous rocks and porphyry copper deposits from the Kerman Cenozoic magmatic arc (SE Iran), and their magmatic–metallogenic implications. Ore geology reviews. Advanced online publication.
- Shahabpour, J., Kramers, J.D., 1987. Lead isotope data from the Sar Cheshmeh porphyry Cu deposit, Kerma, Iran. *Mineralium Deposita* 22, 278–281.
- Shojaat, B., 1992. Geochemical investigations in order to propose possible model for lead–zinc mineralization in the Emarat region. M. Sc. Thesis, Islamic Azad University, North Tehran Branch, Iran (In Farsi).
- Simonetti, A., Gariépy, C., Banic, C., Tanabe, R., Wong, H.K., 2004. Pb isotopic characterization of aircraft-sampled emissions from the Horne smelter at Noranda (Québec) – implications for atmospheric pollution in northeastern North America. *Geochimica et Cosmochimica Acta* 68, 3285–3294.
- Stacey, J.S., Kramers, J.D., 1975. Approximation of terrestrial lead isotope evolution by a two-stage model. *Earth and Planetary Science Letters* 26, 207–221.
- Stampfli, G.M., 2000. Tethyan ocean. In: Bozkurt, E., Winchester, J.A., Piper, J.D.A. (Eds.), *Tectonic and magmatism in Turkey and surrounding area. Special Publication*, vol. 173. Geological Society, London, pp. 1–23.
- Stöcklin, J., 1968. Structural history and tectonics of Iran: a review. *American Association of Petroleum Geologists Bulletin* 52, 1229–1258.
- Stöcklin, J., 1977. Structural correlation of the Alpine ranges between Iran and Central Asia. *Mémoire Hors-Série N° 8 de la Société Géologique de France* 8, 333–353.
- Vanaei, M., 1998. Textural, structural and geochemical characteristics of Emarat Pb–Zn mine (Arak). M. Sc. Thesis, Shahid Bahonar University, Kerman, Iran (In Farsi).
- Verdel, C., 2009. Cenozoic geology of Iran: an integrated study of extensional tectonics and related volcanism. Ph. D. thesis. California Institute of Technology. 287 pp.
- Whitehouse, M.J., 1989. Pb–isotopic evidence for U–Th–Pb behaviour in a prograde amphibolite to granulite facies transition from the Lewisian complex of north-west Scotland: Implications for Pb–Pb dating. *Geochimica et Cosmochimica Acta* 53, 717–724.
- Wrobel-Daveau, J.C., Ringenbach, J.C., Tavakoli, S., Ruiz, G.M.H., Masse, P., de Lamotte, D.F., 2010. Evidence for mantle exhumation along the Arabian margin in the Zagros (Kermanshah area, Iran). *Arabian Journal of Geosciences*. doi:10.1007/s12517-010-0209-z.
- Zamanian, H., 1993. Mineralogy, paragenesis and mode of formation of Hangaran Pb deposit. Malayer. M. Sc. thesis. Tarbiat Moalem University, Tehran (In Farsi).
- Ziserman, A., Momenzadeh, M., 1972. Study on Arak-Esfahan lead–zinc mines. Geological Survey of Iran 60, 16 In Farsi.